Sum Frequency Generation Vibrational Spectroscopy Studies of Protein Adsorption on Oxide-Covered Ti Surfaces

Zoltán Pászti,[†] Jie Wang, Matthew L. Clarke, and Zhan Chen*

Department of Chemistry, University of Michigan, Ann Arbor, Michigan 48109

Received: September 15, 2003; In Final Form: March 24, 2004

Sum frequency generation (SFG) vibrational spectroscopy has been applied to study protein adsorption on native oxide-covered polycrystalline Ti surfaces. We demonstrated that both H_2O_2 solution cleaning and plasma treating can effectively eliminate the unavoidable natural hydrocarbon contamination formed during storage of Ti samples in air. As the presence and potential biological role of this contamination has been a concern of recent studies of inorganic biomaterial interfaces, comparison of the protein adsorption behaviors on the contaminated and cleaned Ti samples has been performed using SFG. Various experiments indicate that hydrocarbon contamination does not greatly affect adsorption of soft proteins on native oxide-covered Ti surfaces. Additional SFG studies show that methyl groups of adsorbed bovine serum albumin have a relatively ordered structure on oxidized Ti, which is slightly affected by the cleaning method. Our data also reveal time-dependent changes of the protein structures during the adsorption process.

1. Introduction

One of the most important processes taking place on foreign surfaces in contact with biological fluids is protein adsorption. The response of living organisms to implanted biomaterials is determined to a great extent by the properties of the initial protein adsorbates. Further interactions including cell adhesion, the inflammatory mechanism, and blood coagulation are initiated and governed by the adsorbed protein layer. Because of its significance in the development of biomaterials and other fields such as food processing or control of biofouling in marine environments, protein adsorption has been extensively studied by various experimental techniques in the last few decades.[1,2]

Recently, sum frequency generation (SFG) vibrational spectroscopy has been successfully developed into a powerful tool to examine various surfaces and interfaces under atmospheric conditions or even in wet environments. SFG is a nonlinear optical process, allowed under the electric-dipole approximation only in media without inversion symmetry. At surfaces or interfaces the inversion symmetry of the bulk is broken and SFG is allowed,[3−24] ensuring the surface/interface sensitivity of the method. SFG provides vibrational spectra of the surface/interface chemical species, allowing the identification and investigation of their orientation distribution and/or surface coverage.[9−29] SFG can also detect interfacial protein structures.[23,24,30−35] The feasibility for gathering ex situ as well as in situ molecular level structural information by SFG from adsorbed proteins on surfaces offers access to data necessary to advance the current empirical understanding of biomaterial−protein interactions.

Due to the combination of excellent mechanical properties and corrosion resistance of its passivating oxide layer, titanium (Ti) is one of the most widely used biomaterials. Large numbers of in vivo studies have demonstrated its biocompatibility and excellent osteointegration properties.[36−39] Accordingly, Ti implants are routinely used with great success in dental practice as well as other implant applications. Despite success in these applications, however, the underlying mechanisms leading to the biocompatible behavior of Ti are still not fully understood.

For example, surface analytical studies revealed that Ti implants prepared according to medical protocols are almost always covered by a few nanometers thick hydrocarbon contamination layer.[40,41] Recent SFG research also shows that hydrocarbon contamination exists on the Ti surface and can be oxidized by UV irradiation.[42] Cell adhesion experiments indicate that hydrocarbon contamination does not substantially affect the osteointegration of Ti unless the amount of contamination is very high.[43] Despite this, we believe that the potential biological effects of contamination in the monolayer range should be addressed. We can elucidate these effects through model studies, for example, through comparison between structures of adsorbed proteins on a cleaned Ti sample and a Ti surface with hydrocarbon contamination.

Due to its importance in the biological response, protein adsorption on Ti has been analyzed by many experimental techniques. It is well established that serum proteins such as bovine serum albumin (BSA) or fibrinogen tend to form a monolayer on Ti samples.[44−46] At the same time, experiments exploring the kinetics or solution concentration dependence of protein adsorption suggest that the adsorption process occurs in two steps.[46−48] A loosely packed protein layer is formed almost immediately after immersion of the substrate into the protein solution. It slowly transforms into a more densely packed monolayer as a result of a change in the orientation and possibly the conformation of the adsorbed molecules. The specifics of such a transformation depend on both the adsorption time and bulk concentration of the protein solution. It is probably worth mentioning, however, that these conclusions are mainly based on indirect observations. A surface-sensitive spectroscopic investigation can provide further details about the rearrangement process of the adsorbed proteins.

* To whom correspondence should be addressed. Fax: (734) 647-4865. E-mail: zhanc@umich.edu.

[†] On leave from the Chemical Research Center of the Hungarian Academy of Sciences, P.O. Box 17, H-1525 Budapest, Hungary.

10.1021/jp0367474 CCC: $27.50
Published on Web 05/18/2004

In this work we will study adsorption of model proteins to Ti samples using SFG. First we will show that the natural hydrocarbon contamination on native oxide-covered Ti surfaces can be eliminated by either a wet (H_2O_2) or a dry (plasma) treatment through SFG studies as well as contact angle measurements. Then we will examine the effect the natural surface contamination has on the adsorption of model proteins including BSA and ubiquitin. Previous studies demonstrated that the SFG spectrum of the C−H stretch region of the adsorbed proteins strongly depends on the substrate properties as well as the environment surrounding the protein molecules.[31−33] Therefore, SFG C−H signals can be used to at least qualitatively identify structural changes in the adsorbed protein layer. Since the contaminated and the hydrocarbon-free native oxide-covered Ti samples have different surface properties, the adsorbed proteins should have different structures and generate different SFG C−H spectra. However, in the present work we found that the C−H spectra of the studied proteins are not significantly influenced by the natural hydrocarbon contamination. Experiments carried out with deuterated ubiquitin seem to suggest that SFG signals of contaminants gradually decreased and finally disappeared. Therefore, we believe that the contamination on Ti surfaces can be replaced by adsorbed protein molecules.

Our SFG studies also revealed that the ordering of the methyl end groups of the hydrophobic side chains of the BSA molecule is very similar on the contaminated and H_2O_2 cleaned substrates, while plasma treatment of Ti leads to a slightly different orientation distribution. In the last part of the paper, we will evaluate the dependence of the orientation distribution of methyl end groups of adsorbed proteins on adsorption time. Our SFG results indicate that structures of adsorbed protein molecules change during the adsorption process.

2. Experimental Details

2.1. Preparation of Ti Layers. Ti films, 100−200 nm thick, were deposited onto glass substrates by electron beam evaporation. The electron beam evaporation was carried out in an oil-free environment at room temperature at pressures lower than $(2-3) \times 10^{-7}$ mbar. We used polished optical glass substrates obtained from HOYA Electronics. The substrates were cleaned by washing in methanol and then etching in a warm mixture of potassium dichromate and sulfuric acid to eliminate hydrocarbon contamination prior to Ti deposition. Ti (99.99%) was purchased from Johnson Matthey. The deposited Ti film thickness was monitored by a quartz crystal oscillator, and the deposition rate was kept around 0.1−0.4 nm/s.

2.2. SFG Measurements. The 20 Hz, 20 ps SFG system used was described in our previous papers,[27−29] and the details will not be repeated here. In the present study we predominantly used the "sample face up" geometry, with an angle of incidence of 60° for the 532 nm visible beam and 53° for the tunable infrared beam. To avoid damaging the Ti layer as well as extensive heating of the sampled area, we had to use reduced visible and infrared pulse energies. The pulse energies for the visible and IR input beams were 10 and 25−30 μJ, respectively. We averaged at least 5−10 individual measurements for all presented spectra. In addition, in all experiments described below at least 2−3 similar samples were prepared and analyzed to make sure that the sample-to-sample repeatability of our measurements was sufficient. All spectra in this paper were normalized by the product of the incoming beam energies measured by separate photodiodes. The nonresonant intensity of a gold reference sample was also recorded prior to each measurement. If comparison between SFG spectra of different samples was necessary, their intensities were scaled together with the help of the corresponding gold reference data.

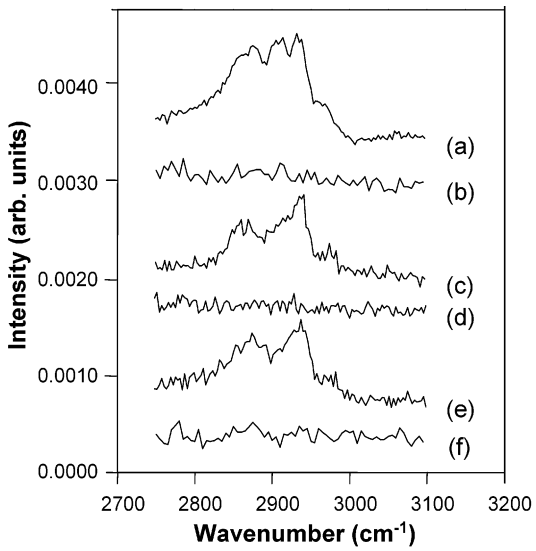

Figure 1. Removal of hydrocarbon contamination from the native oxide-covered titanium surface: SFG spectra collected in the ppp polarization combination from a 100 nm evaporated film after different treatments. Key: (a) as received, (b) 10 min of etching in 40 °C, 5% H_2O_2 solution, (c) the same sample as that of (b), after exposure to the laboratory atmosphere for 20 min, (d) 5 min of glow discharge plasma treatment in 20 Pa of O_2 at a 700 V ac voltage, (e) the same sample as that of (d), after exposure to the laboratory atmosphere for 30 min, (f) a sample similar to that of (d) stored under water for 20 h.

In this work we collected SFG spectra with ssp (s-polarized sum frequency, s-polarized visible, and p-polarized infrared) as well as ppp polarization combinations. We were unsuccessful in detecting reproducible SFG signals in the sps polarization combination, which, considering the Fresnel factors estimated from the published optical constants of bulk Ti,[49] is reasonable.

2.3. Contact Angle Measurements. Static water contact angle measurements were taken using a CAM100 optical contact meter (KSV Instruments). At least four measurements were repeated on each of three similar samples in all experiments.

2.4. Protein Solutions. Fatty acid free BSA was purchased from Sigma. Fully deuterated ubiquitin was obtained from ASLA. BSA and ubiquitin solutions were made by dissolving the proteins in deionized water. The Ti sample was contacted with the protein solution for a certain period of time and then rinsed by water. SFG spectra were collected with the sample in air.

3. Results and Discussion

3.1. Elimination of Hydrocarbon Contamination from the Oxide-Covered Ti Surface. As Ti is one of the most reactive metals, an oxide layer forms almost immediately if a clean Ti surface is exposed to atmospheric conditions. X-ray photoelectron spectroscopy (XPS) and Auger electron spectroscopy (AES) studies demonstrated that this oxide layer is at least a few nanometers thick and consists of TiO_2.[40,41] If a Ti sample is stored in air, this oxide layer is likely to be covered by an adsorbed contamination layer, which contains various hydrocarbons.[40] To study the potential effect of this natural contamination on the protein adsorption properties of Ti samples, we need to prepare hydrocarbon-free, oxide-covered Ti surfaces by removing the contamination layer and using it as a reference.

In Figure 1 we summarize the results of our efforts to prepare a Ti surface without hydrocarbon contamination. Figure 1a

shows a typical ppp-polarized SFG spectrum of an untreated Ti sample. Strong C−H signals clearly indicate that hydrocarbon contamination exists on the surface. The detailed peak assignment is complicated; however, the spectrum is in qualitative agreement with the usual XPS results showing a high amount of CH_2 or CH_3 groups on the surface along with some carbon−oxygen bonds.[40]

In medical practice Ti implants are often cleaned with organic solvents such as acetone, methanol, or ethanol to reduce the hydrocarbon contamination before usage. We will refer to this kind of cleaning as "solvent cleaning". XPS investigations[40] as well as our SFG studies reveal, however, that these treatments are ineffective in completely removing the strongly adsorbed natural hydrocarbon layer. A Ti sample washed in acetone and methanol, for example, gives an SFG spectrum identical to that in Figure 1a. A possible explanation for the strong chemisorption of the contamination is a reaction involving the surface OH groups of the titanium oxide overlayer as discussed in ref 42.

Chemical cleaning of Ti surfaces is also challenging. Most etchants used in the semiconductor industry for cleaning purposes attack Ti very quickly, often causing significant morphological changes on its surface. Solutions containing H_2O_2 at pH lower than 9, however, are known to dissolve Ti at a much slower rate.[50] Previous studies indicated that the etching rate can be controlled by the pH of the solution, which can be adjusted by the addition of NH_4OH.

In our experiments we observed that a warm (40 °C) 5% H_2O_2 solution in water at pH around 8−9 can completely dissolve our 100 nm thick Ti film within a few minutes. Although—according to the SFG measurements—contamination was also removed by this treatment, such a high etching rate is clearly impractical for cleaning purposes. On the other hand, the etchant was ineffective at room temperature. We managed, however, to reduce the etch rate considerably while maintaining the contamination removal efficiency by eliminating NH_4OH from the etchant. Figure 1b shows the SFG spectrum of a 100 nm Ti sample cleaned in a warm 5% H_2O_2 solution for 10 min. After this treatment the contamination SFG signal almost completely disappeared. The surface morphology prior to and after the cleaning was checked by contact mode atomic force microscopy (AFM) measurements with a Molecular Imaging PicoSPM atomic force microscope. AFM measurements revealed no significant sign of sample damage after the cleaning.

Earlier results demonstrated that H_2O_2 facilitates oxidization of the Ti and, at the same time, forms water-soluble complexes with TiO_2,[50] leading finally to the etching effect. Thus, a H_2O_2-etched Ti surface is necessarily covered by an oxide layer which may be slightly thicker than the native oxide. In line with these results, we found that prolonged exposure to the warm H_2O_2 solution leads to formation of a thicker oxide layer (about 20−30 nm, as judged from the appearance of a brown interference color), while the whole Ti film is dissolved after several hours.

Since, due to its orientation sensitivity, SFG cannot always be used alone to determine the surface cleanliness, additional contact angle measurements were carried out to further support the cleaning results. The measurements indicated that while the initial water contact angle on the uncleaned Ti is around 70°, H_2O_2 etching reduces it to below 10°. As the advancing water contact angle is around 30−50° on severely oxidized polymer layers,[51,52] and it is 50° even on carboxyl-terminated self-assembled monolayers,[53] the contact angle results confirm that the H_2O_2 treatment successfully removed the contamination layer. It is important to note, however, that the sample is quickly recontaminated after removal from the etching solution. For example, Figure 1c was collected after the cleaned Ti surface was stored in air for approximately 20 min. The appearance of the strong C−H signals indicates the high affinity of the clean Ti/TiO_2 surface toward atmospheric hydrocarbon contaminants. Water contact angles of the cleaned Ti surface also increase to 30−40° after storage in air for 20 min.

Other methods such as UV irradiation and glow discharge plasma treatment are also promising to remove organic contamination from solid surfaces. Recent SFG research shows that UV irradiation can effectively clean the TiO_2 surface, and the molecular mechanism of such cleaning has been revealed.[42] As far as the plasma treatment is concerned, argon or oxygen plasmas can be used equally well for removing the natural hydrocarbon contamination.[41] XPS and AES results demonstrate that if the plasma-treated surface is exposed to air, it immediately becomes covered by a few nanometers thick stoichiometric TiO_2 layer. Oxygen plasma treatment, naturally, results in the formation of a thicker oxide film.[41]

In our studies we used a homemade plasma cleaner in which the discharge is maintained between two parallel Ti plates using either dc or ac high voltage. SFG measurements indicated that the hydrocarbon contamination can be easily removed by a few minutes of plasma treatment in 10−20 Pa of argon, oxygen, or even air with a 700−1500 V ac voltage. As an example, Figure 1d shows the SFG spectrum of a 100 nm thick Ti layer after a 5 min, 700 V ac plasma treatment in oxygen. The C−H signal is completely eliminated. Recontamination in air is, however, similarly fast as in the case of the H_2O_2 treatment, as demonstrated by Figure 1e, which was taken after the cleaned Ti surface was exposed to air for 30 min. If we put the plasma-cleaned sample immediately into water, the cleanliness can be preserved for a long time as shown by Figure 1f, which was taken 20 h after the cleaning.

Water droplets spread immediately on the plasma-treated sample, indicating the formation of an extremely hydrophilic surface. This result confirms the total removal of hydrocarbon contamination, in good agreement with the SFG results.

Supplementary XPS measurements with an Omicron Nanotechnology (Germany) surface analysis system further support that both the H_2O_2 and plasma treatments successfully eliminate the hydrocarbon contamination. Detailed results will be presented elsewhere, but selected representative data are given as Supporting Information. The findings confirm that if the exposure to the atmosphere is limited to a few seconds, the Ti surface remains remarkably hydrocarbon-free, although it immediately becomes oxidized.

It is interesting to note that a UV-cleaned hydrocarbon-free stoichiometric $TiO_2(110)$ surface exhibits a water contact angle of 40°, while a defective surface (with some Ti^{3+} defects) becomes completely hydrophilic (0° water contact angle).[54] Accordingly, we believe that plasma treatment leads to a hydrocarbon-free surface with highly reactive defect sites, while the H_2O_2 treatment results in a somewhat more perfect, less reactive titanium oxide surface. This conclusion is also confirmed by our preliminary XPS results.

3.2. Protein Adsorption on Hydrocarbon-Contaminated and Cleaned Oxide-Covered Ti Surfaces. It was mentioned earlier that the surface of Ti implants used in medical practice is usually covered by a natural hydrocarbon contamination layer. Therefore, it is interesting to study how this contamination interacts with plasma proteins. Here we will address this question by analyzing SFG spectra of model proteins on uncleaned and hydrocarbon-contamination-free Ti samples.

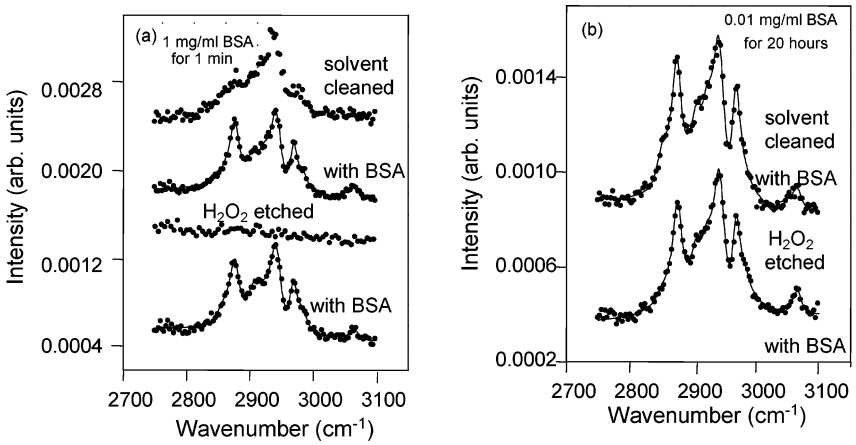

Figure 2. ppp-polarized SFG spectra of BSA adsorbed from (a) a 1 mg/mL solution for 1 min and (b) a 0.01 mg/mL solution for 20 h on solvent-cleaned and H_2O_2-etched Ti surfaces. The first, second, third, and fourth curves from the top in (a) represent the spectra of the solvent-cleaned Ti, the solvent-cleaned Ti contacted with BSA solution, the H_2O_2-etched Ti, and the H_2O_2-etched Ti contacted with BSA solution, respectively. In (b) the first curve from the top was measured on the solvent-cleaned Ti contacted with BSA solution, while the second is the spectrum of BSA on H_2O_2-etched Ti. Dots are experimental data, and lines are fitted spectra.

TABLE 1: Fitting Parameters of the Methyl Vibrations Obtained from the Analysis of the SFG Spectra in Figure 2

	symmetric CH_3, $\omega \approx 2875$ cm^{-1}, $\Gamma \approx 9$ cm^{-1}		Fermi resonance, $\omega \approx 2940$ cm^{-1}, $\Gamma \approx 11$ cm^{-1}		asymmetric CH_3, $\omega \approx 2965$ cm^{-1}, $\Gamma \approx 8$ cm^{-1}	
sample	abs val[a]	phase[b] (deg)	abs val[a]	phase[b] (deg)	abs val[a]	phase[b] (deg)
1 mg/mL BSA for 1 min on solvent-cleaned Ti	0.086	106	0.15	118	0.072	91
1 mg/mL BSA for 1 min on H_2O_2-cleaned Ti	0.079	110	0.14	119	0.071	91
0.01 mg/mL BSA for 20 h on solvent-cleaned Ti	0.075	107	0.13	118	0.071	98
0.01 mg/mL BSA for 20 h on H_2O_2-cleaned Ti	0.072	107	0.12	111	0.065	94

[a] Absolute value of the complex fitting amplitude: in arbitrary units. The estimated error of the amplitudes is 5−8%. [b] The total uncertainity of the phase values is 2−4°.

Figure 2a shows ppp SFG spectra in the C−H stretch region of solvent-cleaned (i.e., still hydrocarbon-contaminated) and H_2O_2-etched Ti samples before and after BSA adsorption from a 1 mg/mL solution. Figure 2b shows similar spectra after protein adsorption from a 0.01 mg/mL BSA solution. The spectra of all the BSA-contacted samples are strikingly different from that of the solvent-cleaned sample, indicating that even in a short time significant BSA adsorption took place. On the other hand, all BSA-containing samples exhibit a qualitatively similar spectrum. The strong structures around 2875, 2940, and 2965 cm^{-1} can be attributed to different vibration modes of the methyl groups. Weaker bands around 2850 and 2920 cm^{-1} are due to methylene stretches, while the structure around 3060 cm^{-1} is assigned to vibrations of aromatic groups. The presence of the aromatic groups confirms that protein adsorption took place as aromatic SFG signals are missing from the spectrum of the contamination layer.

A more quantitative comparison of the spectra is possible if we fit them with the usual model function $I(\omega_{IR}) \propto |A_{NR} + \sum_v [A_v/(\omega_{IR} - \omega_v + i\Gamma_v)]|^2$, where $I(\omega_{IR})$ is the sum frequency intensity as a function of the infrared frequency ω_{IR}, A_{NR} is the amplitude of the nonresonant background, A_v is the fitting amplitude, ω_v is the frequency, and Γ_v is the width of the vth molecular vibration. The parameters A_v can be regarded as the products of the relevant vibration amplitudes (which are related to the orientation distribution, surface density, and molecular hyperpolarizability) and the Fresnel factors (for further details, see ref 3 or 26). We have to take into account, however, that, in the case of a metal substrate, both the nonresonant background and the Fresnel factors are complex numbers. Accordingly, the fitting amplitudes appearing in the above expression will also be complex. Taking into account that for ordinary SFG measurements the absolute phase information is lost, it is easy to see that in the case of the ssp polarization combination, where only one second-order surface susceptibility tensor element (i.e., χ_{yyz}) contributes to the spectrum in our experimental conditions, we can fit the spectrum with a complex nonresonant background and real fitting amplitudes for the resonant peaks. On the contrary, in the case of the ppp polarization combination two independent tensor elements (χ_{xxz}, which is equal to χ_{yyz}, and χ_{zzz}, both weighted by the appropriate Fresnel factors and local field correction factors) give contributions in our experimental geometry. Thus, for the fitting of the ppp spectra we can use a real nonresonant background and complex resonant peaks, as indicated, for example, in ref 11. For further details see the Supporting Information.

Our fitting procedure included methyl, methylene, and aromatic vibrations. The fitting results for the methyl vibrations of Figure 2 are summarized in Table 1. The data also confirm the similarity of the BSA-related spectra in Figure 2, regardless of the bulk BSA concentration, adsorption time, or surface cleanliness. This suggests that the natural hydrocarbon contamination may not substantially affect the structure and properties of the adsorbed BSA molecules.

To further clarify this point, we repeated the experiment with a fully deuterated protein. As we were unable to find fully deuterated BSA, we used fully deuterated ubiquitin instead. Since our model protein is fully deuterated, any interference between the hydrocarbon contamination and protein-related signals is eliminated; thus, it is possible to study separately the structure of the hydrocarbon layer and the adsorbed protein molecules.

In Figure 3a we present the ppp SFG spectra of *d*-ubiquitin adsorbed onto a solvent-cleaned and a H_2O_2-cleaned evaporated Ti sample in the C−D stretch region. The spectra, closely resembling the case of the C−H region of BSA, are very similar.

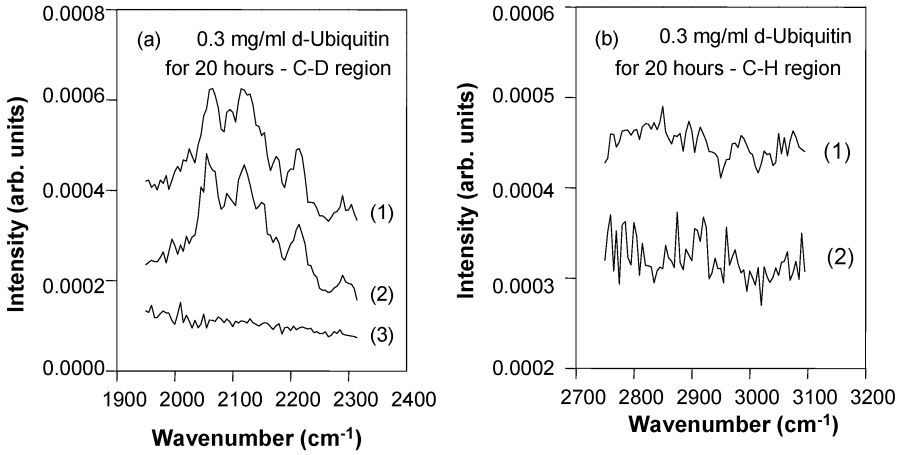

Figure 3. Adsorption of totally deuterated ubiquitin on evaporated titanium substrates cleaned with different techniques from a 0.3 mg/mL solution for 20 h: (a) C−D region, (1) solvent-cleaned, (2) H_2O_2-etched, (3) solvent-cleaned, before protein adsorption; (b) C−H region, (1) solvent-cleaned, (2) H_2O_2-etched substrate with deuterated ubiquitin. All spectra are in the ppp polarization combination.

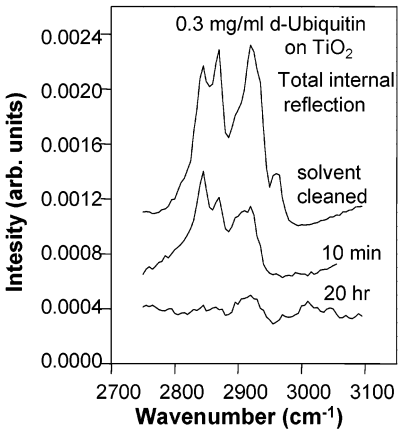

Figure 4. Effect of the adsorption of deuterated ubiquitin on the contamination signal from a solvent-cleaned TiO_2 substrate: (top curve), C−H region before protein adsorption, (middle curve) C−H region after 10 min of adsorption from a 0.3 mg/mL solution, (bottom curve) C−H region after 20 h of adsorption from a 0.3 mg/mL solution. All spectra are in the ppp polarization combination and were taken in the total internal reflection geometry.

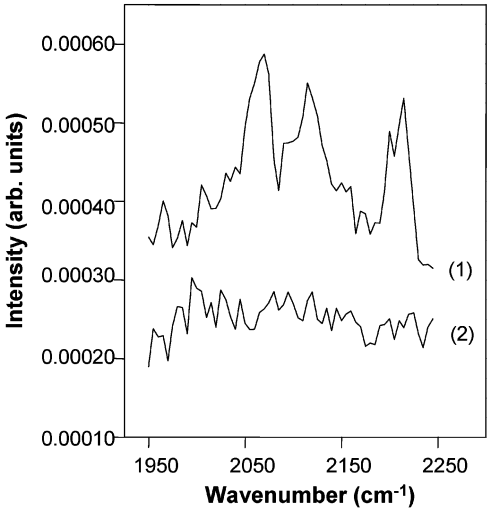

Figure 5. Desorption of deuterated butanol from a plasma-cleaned Ti surface in water: (1) C−D stretch region of a *d*-butanol-contaminated plasma-cleaned Ti sample, (2) C−D region of the same sample after 2 h of exposure to water. Both spectra are in the ppp polarization combination.

The SFG spectra of the same samples in the C−H stretch region are shown in Figure 3b. Interestingly, there is hardly any C−H signal even in the case of the solvent-cleaned sample after protein adsorption. This suggests that either the methyl and methylene groups in the contamination molecules would adopt a totally random distribution under the protein film or they desorb during protein adsorption.

To check the behavior of the contamination C−H signals during adsorption of *d*-ubiquitin, we repeated the above experiment in the total reflection geometry (see the Supporting Information), where the SFG signals can be enhanced by several orders of magnitude.[11,19] The spectra were collected from the substrate/air interface of a transparent TiO_2 sample after exposure to a *d*-ubiquitin solution for certain times. The results indicate that the contamination-related C−H signal decreased noticeably after 10 min of exposure to the *d*-ubiquitin solution and almost completely disappeared after 20 h (Figure 4).

In a separate experiment we intentionally contaminated a plasma-cleaned Ti sample with deuterated 1-butanol, which is believed to bond to the TiO_2 surface via hydrogen bonding and is used sometimes in medical practice to increase the hydrophobicity of the Ti implant.[55] As can be seen in Figure 5, the *d*-butanol layer was completely dissolved upon immersing the sample into water. Similar behavior was found in BSA solution. This observation supports the possibility of contamination desorption during protein adsorption.

Our studies with ubiquitin indicate that, like BSA, ubiquitin also rapidly forms an adsorbed layer on solid surfaces. According to previous experience with polymers[22,29] or proteins,[31,32] randomization processes due to changes in the local environment are expected to be fast. Therefore, we expect the almost immediate disappearance of the C−H-related contamination signal upon contacting the sample with the *d*-ubiquitin solution. Instead, we found a relatively slow kinetic process occurred, which is in favor of a gradual replacement process.

Replacement of the hydrocarbon contamination by protein molecules during adsorption can explain the similarity of the protein-related SFG spectra collected from solvent-cleaned and H_2O_2-etched Ti surfaces. In addition, it is in line with the lack of any strong indication for the role of the natural hydrocarbon contamination in cell-level biological experiments. According to this result, the C−H vibrations observed in the BSA-contacted samples can be identified as signals predominantly coming from the albumin molecules, regardless of whether the substrate was originally clean or contaminated.

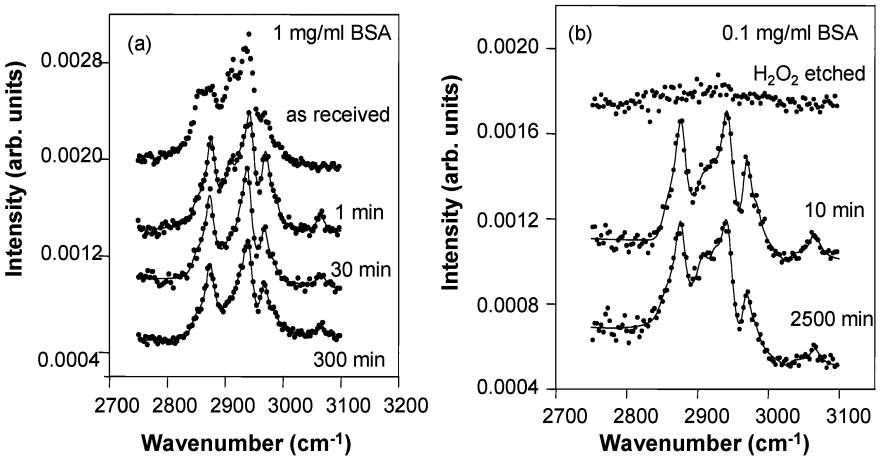

Figure 6. (a) BSA adsorbed on solvent-cleaned Ti from a 1 mg/mL solution for 1, 30, and 300 min. (b) BSA adsorbed on H_2O_2-etched Ti from a 0.1 mg/mL solution for 10 and 2500 min. All spectra were taken in the ppp polarization combination. Dots are experimental data, and lines are fitted spectra.

TABLE 2: Fitting Parameters of the Methyl Vibrations Obtained from the Analysis of the SFG Spectra in Figure 6

	symmetric CH_3, $\omega \approx 2875$ cm^{-1}, $\Gamma \approx 9$ cm^{-1}		Fermi resonance, $\omega \approx 2940$ cm^{-1}, $\Gamma \approx 11$ cm^{-1}		asymmetric CH_3, $\omega \approx 2965$ cm^{-1}, $\Gamma \approx 8$ cm^{-1}	
sample	abs val[a]	phase[b] (deg)	abs val[a]	phase[b] (deg)	abs val[a]	phase[b] (deg)
1 mg/mL BSA on solvent-cleaned Ti (Figure 6a)						
for 1 min	0.094	105	0.145	115	0.085	94
for 30 min	0.087	107	0.14	113	0.063	95
for 300 min	0.092	101	0.145	112	0.064	94
0.1 mg/mL BSA on H_2O_2-cleaned Ti (Figure 6b)						
for 10 min	0.073	106	0.115	110	0.063	91
for 2500 min	0.071	110	0.12	117	0.042	94

[a] Absolute value of the complex fitting amplitude: in arbitrary units. The estimated error of the amplitudes is 5−8%. [b] The total uncertainity of the phase values is 2−4°.

A question arises if we believe that hydrocarbon contamination on Ti surfaces is replaced by protein molecules: why such contamination cannot be replaced by organic solvents (i.e., why the solvent-cleaning method is not effective). We cannot completely address this question here. According to our SFG studies, the SFG spectra collected from the solvent-cleaned Ti surfaces are identical to those collected from Ti surfaces before the solvent cleaning. Perhaps, partial replacement of the hydrocarbon contamination occurred. However, the surface structures of the contamination layer on Ti are still similar before and after such partial replacements, and thus, SFG spectra are identical.

3.3. Adsorption Time Dependence of BSA Adsorption on Ti. As a next step, we have studied the effect of the adsorption time on the properties of the adsorbed BSA layer. The behavior of the protein molecules on the solvent-cleaned and H_2O_2-etched substrates was very similar, further confirming that the natural hydrocarbon contamination would not substantially affect protein adsorption. SFG spectra collected from adsorbed proteins on the plasma-cleaned samples, however, suggest slightly different adsorption properties, which will be discussed separately.

As an example, in Figure 6a we present ppp SFG spectra of BSA adsorbed from a 1 mg/mL solution onto solvent-cleaned Ti for different times. Figure 6b shows similar spectra collected on H_2O_2-etched substrates after adsorption from a 0.1 mg/mL solution. Although the main features of the spectra of the samples prepared using 0.1 and 1 mg/mL solutions are qualitatively similar, there is an adsorption-time-dependent change in both cases: the relative intensity of the asymmetric methyl peak around 2965 cm^{-1} clearly decreases with increasing adsorption time. This effect is confirmed also by the fitting results (Table 2): $|A_{as}|/|A_s|$ decreases from ~0.9 to 0.6−0.7 in both cases.

We believe that the observed SFG spectra are related to the molecular structures of the adsorbed proteins. As we mentioned earlier, the spectrum measured in the ppp polarization combination reflects the weighted sum of the χ_{xxz} and χ_{zzz} nonlinear susceptibility tensor elements. An uncontrolled change of the substrate surface optical properties, therefore, could result in some spectral changes via modification of the weighting factors (Fresnel factors). The spectral differences in Figure 6 are, however, not due to differences between the weighting factors for different samples. The solvent-cleaned substrates used in the experiment are identical; the time-dependent changes of the adsorbed protein SFG signals on such identical substrates cannot be attributed to the potential differences of the surface optical properties. On the other hand, independent measurements demonstrate that BSA forms a monolayer on oxide-covered Ti surfaces,[44−46] which means that thin-film-related effects can also be ruled out. Finally, it was demonstrated that the nonlocal contributions to the SFG signal, which may well affect the ppp SFG spectrum, are relatively insensitive to changes in the structure of the adsorbed protein layer.[56] Therefore, the spectral differences observed in Figure 6 should be caused by structural variations of adsorbed protein molecules.

To elucidate the possible reason for the observed spectral changes in Figure 6, we carried out simple model calculations in which we evaluated the expected asymmetric-to-symmetric methyl peak ratio in the ppp spectrum for different Gaussian-type orientation distribution functions using the published optical constants for Ti.[49] Fresnel factor calculations indicate that—due

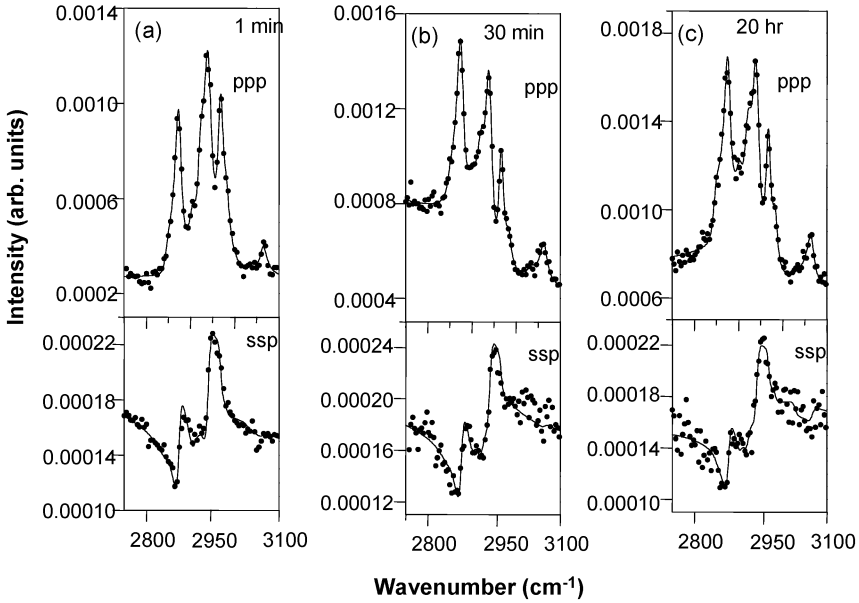

Figure 7. SFG spectra of BSA adsorbed on plasma-cleaned Ti measured in the ppp and ssp polarization combinations: (a) 1 min, (b) 30 min, and (c) 20 h of adsorption time from a 1 mg/mL solution. Dots are experimental data, and lines are fitted spectra.

TABLE 3: Fitting Parameters of the Methyl Vibrations Obtained from the Analysis of the SFG Spectra in Figure 7

	symmetric CH_3, $\omega \approx 2875$ cm^{-1}, $\Gamma \approx 9$ cm^{-1}			Fermi resonance, $\omega \approx 2940$ cm^{-1}, $\Gamma \approx 11$ cm^{-1}			asymmetric CH_3, $\omega \approx 2965$ cm^{-1}, $\Gamma \approx 8$ cm^{-1}		
	ppp		ssp	ppp		ssp	ppp		ssp
sample	$\lvert A_s\rvert$[a]	phase[b] (deg)	A_s[a]	$\lvert A_{FR}\rvert$[a]	phase[b] (deg)	A_{FR}[a]	$\lvert A_{as}\rvert$[a]	phase[b] (deg)	A_{as}[a]
1 mg/mL BSA on plasma-cleaned Ti									
for 1 min	0.11	108	0.025	0.147	112	0.03	0.1	96	−0.009
for 30 min	0.091	113	0.021	0.14	119	0.025	0.072	94	−0.005
for 20 h	0.092	112	0.02	0.145	117	0.025	0.078	94	−0.006

[a] Absolute value of the complex fitting amplitude for the ppp polarization combination and value of the real fitting amplitude for the ssp polarization combination: in arbitrary units. The estimated error of the amplitudes is 5−10%. [b] The total uncertainity of the phase values is 2−4°.

to the weighting factors—the ppp SFG spectrum is dominated by the *zzz* susceptibility tensor component. The calculations were based on the standard expressions for the surface second-order nonlinear susceptibility due to methyl groups.[26,57−60] Further details are given as Supporting Information.

It is worth noting that, according to our knowledge about the complex structure of the BSA molecule, probably only a certain fraction of the methyl end groups on the hydrophobic side chains contribute to the SFG spectra. The other methyl groups, situated in locally centrosymmetric environments, may be invisible for SFG. Thus, the distribution function deduced from the SFG spectra contains information only about those methyl groups in noncentrosymmetric environments, while the other methyl groups can be described by a random distribution. The percentage of the randomly distributed methyl groups could be estimated by simultaneous measurements of the absolute SFG intensity and the surface concentration of the BSA molecules. While such a measurement is out of the scope of the present work, changes in the distribution function of methyl groups accessible for SFG are still indicative of structural rearrangement of the BSA molecules during adsorption.

Although it is difficult to give an accurate estimation of the actual orientation distribution function of the methyl groups contributing to the SFG spectra, the calculation results indicate that the observed time-dependent decrease of the asymmetric-to-symmetric methyl peak ratio can be explained by the narrowing of an orientation distribution centered around the surface normal. Qualitatively, narrowing of the methyl distribution can be related to conformational changes in the protein molecule. A broader distribution suggests that the adsorbed BSA molecules tend to "spread" on the surface, exhibiting a more open structure, while the narrowing can be explained by the formation of a more closely packed layer containing more "compact" molecules. Accordingly, we conclude that as the adsorption time lengthens the methyl orientation distribution narrows, indicating a more ordered protein layer. This result is confirmed by earlier studies, where time-dependent reorientation of protein molecules was proposed on the basis of the measured kinetics of adsorption.[46−48]

3.4. BSA Adsorption on Plasma-Treated Ti. Figure 7 shows ssp and ppp SFG spectra of BSA adsorbed from 1 mg/mL solution onto plasma-cleaned evaporated Ti for different times. The spectra look again quite similar, which is confirmed by the fitting results (Table 3). Interestingly, although the relative strength of the asymmetric methyl peak in the ppp polarization combination again decreases with increasing adsorption time, it remains considerably high ($|A_{as}|/|A_s| \approx 0.85$) even after a long time, in contrast to what was found on the solvent-cleaned or H_2O_2-treated Ti ($|A_{as}|/|A_s| \approx 0.6-0.7$). This suggests that the SFG active methyl groups of BSA adsorbed on the plasma-cleaned Ti surface are always a little more disordered than those on the solvent-cleaned Ti. The possible reason is that the plasma-treated surface is more reactive as already mentioned in section 3.1, and can form some very strong bonds with the adsorbed protein molecules, thus stabilizing a relatively open structure. Perhaps this observation can be related to recent results indicating that cell adhesion is enhanced on plasma-treated Ti surfaces.[61]

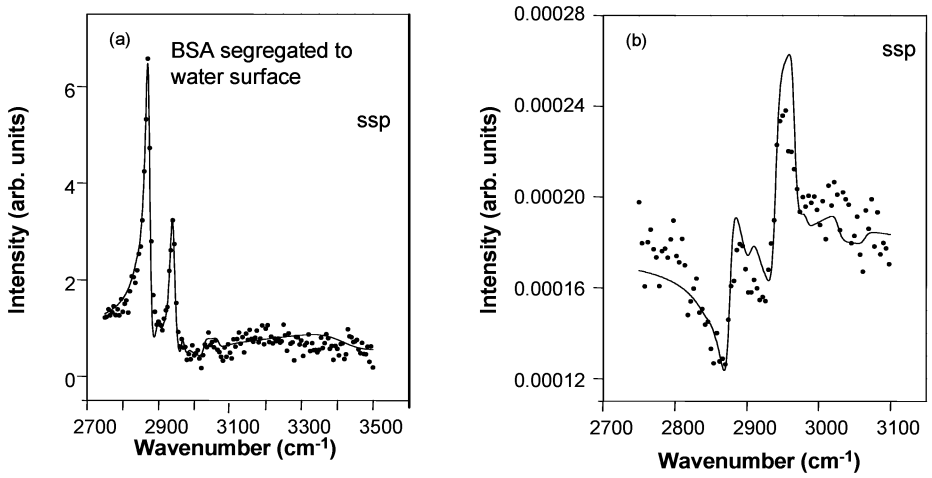

Figure 8. (a) SFG spectrum of BSA segregated to the surface of a 1 mg/mL solution measured in the ssp polarization combination: (●) measured data, (—) fitting result. (b) ssp-polarized SFG spectrum of BSA adsorbed from a 1 mg/mL solution onto plasma-cleaned Ti in 30 min (●) and the scaled fitting result from (a) with the nonresonant background of Ti (—).

As the ssp signal probes the *yyz* susceptibility tensor component alone, the asymmetric-to-symmetric methyl stretch peak amplitude ratio should not be influenced by uncontrolled changes of the optical properties of the substrate. Thus, it is worthwhile to compare the ssp data with the results obtained from the above model calculation from ppp data. Fitting indicates that the ssp spectra can be described by a strong symmetric methyl stretch and Fermi resonance, along with some methylene contributions. In contrast to the ppp spectra, the asymmetric methyl peak in the ssp spectra is always very weak. According to the model calculation, the small asymmetric-to-symmetric methyl peak amplitude ratio is compatible with a relatively narrow ($\sigma \approx 20°$) distribution centered around the sample surface normal. More tilted or broader distributions should lead to higher asymmetric methyl amplitudes. The distribution of BSA methyl groups on the plasma-treated Ti surface is somewhat broader ($\sigma \approx 30°$). This result is in agreement with the conclusions obtained from the analysis of the ppp spectra.

In previous SFG experiments it was demonstrated that the methyl groups in a BSA monolayer that segregate to the surface of a BSA solution exhibit a very broad orientation distribution, which was indicated by a high asymmetric-to-symmetric methyl peak amplitude ratio in the ssp spectra.[34] Figure 8a shows the ssp spectrum collected from the BSA monolayer at the BSA solution/air interface with a BSA solution concentration of 1 mg/mL. Although it is not immediately evident (due to the different phases of the asymmetric stretch and the Fermi resonance), fitting reveals that this spectrum contains a strong symmetric methyl stretch and Fermi resonance as well as a quite intense asymmetric methyl peak along with some methylene signals. Figure 8b shows the ssp spectrum of BSA adsorbed on plasma-cleaned Ti along with a calculated spectrum obtained by combining the fitting result of BSA at the solution/air interface (Figure 8a) and the nonresonant background of Ti acquired from Figure 7b. Although the general shapes of the measured (BSA on plasma-cleaned Ti) and the calculated (BSA at the solution/air interface with the same nonresonant background as BSA on plasma-cleaned Ti) spectra are similar, there are significant differences, especially around 2950−3000 cm^{-1}. Further calculations show that the intensity of the calculated spectrum is higher predominantly because of the larger asymmetric methyl contribution in the SFG spectrum of BSA on water. This result indicates that the conformation of BSA is different on water and Ti surfaces and emphasizes how the different environment influences the structure of protein molecules.

4. Conclusions

In this work, using native oxide-covered Ti as a model substrate, we successfully demonstrated that SFG can be used to collect molecular level information about protein adsorption on metallic biomaterials. One of the major difficulties in handling Ti in air is that its oxidized surface is very easily contaminated by a hydrocarbon layer from the atmospheric environment. To deal with this issue, we showed that both a wet chemical treatment (using a H_2O_2 solution) and a dry technique (glow discharge plasma treatment) can remove the contamination.

A comparative SFG study of adsorption of model proteins such as BSA and ubiquitin on the hydrocarbon-free and -contaminated Ti surfaces revealed that protein molecules have similar structures on the surfaces, evidenced by the similar structures of the methyl groups on the hydrophobic side chains of the adsorbed protein molecules deduced by SFG. Supporting experiments suggested that the contamination is replaced by the protein molecules during the adsorption process, and therefore does not substantially affect the adsorbed protein structure.

A qualitative evaluation of the measured SFG spectra of BSA adsorbed on Ti indicated that the orientation distribution of the methyl groups is relatively narrow and centered around the surface normal. Using SFG, we also followed the kinetics of protein adsorption on oxide-covered Ti surfaces. Our results demonstrated that adsorbed BSA molecules change conformation during the adsorption process.

Acknowledgment. This work is supported by the National Science Foundation (NATO postdoctoral fellowship for Dr. Zoltán Pászti, Grant No. DGE-0209532), the start-up fund from the University of Michigan, the Office of Naval Research (Grant No. N00014-02-1-0832), and the Beckman Foundation. We are grateful to Dr. Ovidiu Toader (Michigan Ion Beam Laboratory, University of Michigan, Ann Arbor, MI) and Dr. György Molnár (Research Institute for Technical Physics and Materials Science, Budapest, Hungary) for their help in the preparation of the Ti samples.

Supporting Information Available: Details about the XPS results, SFG spectral fitting, and SFG data (PDF). This material is available free of charge via the Internet at http://pubs.acs.org.

References and Notes

(1) Horbett, T. A.; Brash, J. L. *Proteins at Interfaces II, Fundamentals and Applications*; ACS Symposium Series 602; American Chemical Society: Washington, DC, 1995.

(2) Brash, J. L.; Horbett, T. A. *Proteins at Interfaces, Physicochemical and Biochemical Studies*; ACS Symposium Series 343; American Chemical Society: Washington, DC, 1987.

(3) Shen, Y. R. *The Principles of Nonlinear Optics*; Wiley: New York, 1984.

(4) Shen, Y. R. *Nature* **1989**, *337*, 519.

(5) Miranda, P. B.; Shen, Y. R. *J. Phys. Chem. B* **1999**, *103*, 3292.

(6) Bain, C. D. *J. Chem. Soc., Faraday Trans.* **1995**, *91*, 1281.

(7) Eisenthal, K. B. *Chem. Rev.* **1996**, *96*, 1343.

(8) Gragson, D. E.; Richmond, G. L. *J. Phys. Chem. B* **1998**, *102*, 3847.

(9) Walker, R. A.; Gruetzmacher, J. A.; Richmond, G. L. *J. Am. Chem. Soc.* **1998**, *120*, 6991.

(10) Conboy, J. C.; Messmer, M. C.; Richmond, G. L. *J. Phys. Chem.* **1996**, *100*, 7617.

(11) Williams, C. T.; Yang, Y.;, Bain, C. D. *Langmuir* **2000**, *16*, 2343.

(12) Gracias, D. H.; Chen, Z.; Shen, Y. R.; Somorjai, G. A. *Acc. Chem. Res.* **1999**, *320*, 930.

(13) Chen, Z.; Ward, R.; Tian, Y.; Baldelli, S.; Opdahl, A.; Shen, Y. R.; Somorjai, G. A. *J. Am. Chem. Soc.* **2000**, *122*, 10615.

(14) Shultz, M. J.; Schnitzer, C.; Simonelli, D.; Baldelli, S. *Int. Rev. Phys. Chem.* **2000**, *19*, 123.

(15) Pizzolatto, R. L.; Yang, Y. J.; Wolf, L. K.; Messmer, M. C. *Anal. Chim. Acta* **1999**, *397*, 81.

(16) Kim, J.; Cremer,P. S. *J. Am. Chem. Soc.* **2000**, *122*, 12371.

(17) Briggman, K. A.; Stephenson, J. C.; Wallace, W. E.; Richter, L. J. *J. Phys. Chem. B* **2001**, *105*, 2785.

(18) Gautam, K. S.; Schwab, A. D.; Dhinojwala, A.; Zhang, D.; Dougai, S. M.; Yeganeh, M. S. *Phys. Rev. Lett.* **2000**, *85*, 3854.

(19) Löbau, J.; Wolfrum, K. *J. Opt. Soc. Am. B* **1997**, *14*, 2505.

(20) Scatena, L. F.; Brown, M. G.; Richmond, G. L. *Science* **2001**, *292*, 908.

(21) Chen, Z.; Shen, Y. R.; Somorjai, G. A. *Annu. Rev. Phys. Chem.* **2002**, *53*, 437.

(22) Wang, J.; Woodcock, S. E.; Buck, S. M.; Chen, C. Y.; Chen, Z. *J. Am. Chem. Soc.* **2001**, *123*, 9470.

(23) Chen, Z.; Ward, R.; Tian, Y.; Shen, Y. R.; Somorjai, G. A. *J. Biomed. Mater. Res.* **2002**, *62*, 254.

(24) Kim, J.; Cremer, P. S. *Chem. Phys. Chem.* **2001**, *2*, 543.

(25) Hirose, C.; Akamatsu, N.; Domen, K. *Appl. Spectrosc.* **1992**, *46*, 1051.

(26) Zhuang, X.; Miranda, P. B.; Kim, D.; Shen, Y. R. *Phys. Rev. B* **1999**, *59*, 12632.

(27) Wang, J.; Chen, C. Y.; Buck, S. M.; Chen, Z. *J. Phys. Chem. B* **2001**, *105*, 12118.

(28) Chen, C. Y.; Wang, J.; Woodcock, S. E.; Chen, Z. *Langmuir* **2002**, *18*, 1302.

(29) Wang, J.; Paszti, Z.; Even, M. A.; Chen, Z. *J. Am. Chem. Soc.* **2002**, *124*, 7016.

(30) Kim, G.; Gurau, M.; Kim, J.; Cremer, P. S. *Langmuir* **2002**, *18*, 2807.

(31) Wang, J.; Buck, S. M.; Even, M. A.; Chen, Z. *J. Am. Chem. Soc.* **2002**, *124*, 13302.

(32) Wang, J.; Buck, S. M.; Chen, Z. *J. Phys. Chem. B* **2002**, *106*, 11666.

(33) Kim, J.; Somorjai, G. A. *J. Am. Chem. Soc.* **2003**, *125*, 3150.

(34) Wang, J.; Buck, S. M.; Chen, Z. *Analyst* **2003**, *128*, 773.

(35) Koffas, T. S.; Kim, J.; Lawrence, C. C.; Somorjai, G. A. *Langmuir* **2003**, *19*, 3563.

(36) Williams, D. F. *Fundamental Aspects of Biocompatibility*; CRC Press: Boca Raton, FL, 1981; Vol. 1.

(37) Brånemark, P. I.; Zarb, G. A.; Albrektsson, T. *Tissue Integrated Protheses: Osseointegration in Clinical Practice*; Quintessence: Chicago, 1985.

(38) Johansson, C. B.; Hansson, H. A.; Albrektsson, T. *Biomaterials* **1990**, *11*, 276.

(39) Kasemo, B. *Surf. Sci.* **2002**, *500*, 656.

(40) Lausmaa, J. *J. Electron Spectrosc. Relat. Phenom.* **1996**, *81*, 343.

(41) Aronsson, B. O.; Lausmaa, J.; Kasemo, B. *J. Biomed. Mater. Res.* **1997**, *35*, 49.

(42) Wang, C. Y.; Groenzin, H.; Shultz, M. J. *Langmuir* **2003**, *19*, 7330.

(43) Keller, J. C.; Wick, D. G.; Draughn, R. A.; Wightman, J. P. *J. Adhes.* **1995**, *54*, 145.

(44) Williams, R. L.; Williams, D. F. *Biomaterials* **1988**, *9*, 206.

(45) Nakanishi, K.; Sakiyama, T.; Imamura, K. *J. Biosci. Bioeng.* **2001**, *91*, 233.

(46) Jackson, D. R.; Omanovic, S.; Roscoe, S. G. *Langmuir* **2000**, *16*, 5449.

(47) Hughess Wassell, D. T.; Embery, G. *Biomaterials* **1996**, *17*, 859.

(48) Giacomelli, C. E.; Esplandiú, M. J.; Ortiz, P. I.; Avena, M. J.; De Pauli, C. P. *J. Colloid Interface Sci.* **1999**, *218*, 404.

(49) Palik, E. D., Ed. *Handbook of Optical Constants of Solids*; Academic Press: Orlando, FL, 1985.

(50) van den Meerakker, J. E. A. M.; Metsemakers, J. P.; Giesbers, J. B. *J. Electrochem. Soc.* **2002**, *149*, C256.

(51) Cho, J.-S.; Kim, K.-H.; Han, S.; Beag, Y.-W.; Koh, S.-K. *Prog. Org. Coat.* **2003**, *48*, 251.

(52) Balazs, D. J.; Triandafillu, K.; Wood, P.; Chevolot, Y.; van Delden, C.; Harms, H.; Hollensteind, C.; Mathieu, H. J. *Biomaterials*, in press.

(53) Faucheux, N.; Schweiss, R.; Lützow, K.; Werner, C.; Groth, T. *Biomaterials*, in press.

(54) Wang, R.; Sakai, N.; Fuyishima, A.; Watanabe, T.; Hashimoto, K. *J. Phys. Chem. B* **1999**, *103*, 2188

(55) Nygren, H. *Colloids Surf., B* **1996**, *6*, 329.

(56) Wang, J.; Pászti, Z.; Even, M. A.; Chen, Z. *J. Phys. Chem. B* **2004**, *108*, 3625.

(57) Hirose, C.; Akamatsu, N.; Domen, K. *J. Chem. Phys.* **1992**, *96*, 997.

(58) Oh-e, M.; Lvovsky, A. I.; Wei, X.; Shen, Y. R. *J. Chem. Phys.* **2000**, *113*, 8827.

(59) Gautam, K. S.; Dhinojwala, A. *Macromolecules* **2001**, *34*, 1137.

(60) Hirose, C.; Yamamoto, H.; Akamatsu, N.; Domen, K. *J. Phys. Chem.* **1993**, *97*, 10064

(61) Shibata, Y.; Hosaka, M.; Kawai, R.; Miyazaki, K. *Int. J. Oral Max. Impl.* **2002**, *17*, 771.